FIDELITY MANAGEMENT OF AEROTHERMODYNAMIC MODELLING FOR DESTRUCTIVE RE-ENTRY

Fábio Morgado, Sai Abhishek Peddakotla, Catarina Garbacz, Massimiliano Vasile and Marco Fossati

Aerospace Centre of Excellence, University of Strathclyde, Glasgow, G1 1XJ, United Kingdom

ABSTRACT

The re-entry process is distinguished by the presence of several fragments with intricate geometries resulting from the demise process, which may lead to complex features in the re-entry flow. An example of these features is shock impingement, which leads to highly localized loading of pressure and heat flux on the bodies' surface. These loads impact the overall dynamics and cannot be captured using state-of-the-art low-fidelity approaches.A multi-fidelity approach is considered to reduce the uncertainty in predictions during a multiple body re-entry. Such an approach allows the usage of low-fidelity models along with high-fidelity methods such as Computational Fluid Dynamics or Direct Simulation Monte Carlo. This research investigates the formulation and use of a strategy for the automatic selection of the level of fidelity in the computation of aerothermodynamic loads acting on bodies undergoing destructive atmospheric re-entry. Based on the Billig formula, which provides an approximation for the definition of a shock-wave envelope for blunt bodies, a criterion to automatically detect when to transition from low-to-high/high-to-low fidelity is proposed. In the present work, the focus will be on the application of a shock-envelope logic to switch between fidelity methods, exploring the influence of the shock waves from leading fragments onto the following fragments.

Index Terms— Re-entry, Multi-fidelity, Fragmentation

1. INTRODUCTION

Space sustainability is at risk due to the increasing number of man-made satellites. To avoid the cluttering of space and decrease the risk of in-orbit collisions, they must be disposed of after reaching their end of life. An effective solution to this problem is to make the satellites undergo destructive atmospheric re-entry, either controlled or uncontrolled, through which the satellite breaks into several fragments that are required to be demised. An additional challenge is to guarantee that fragments with impact kinetic energy greater than 15 Joules should have a human casualty risk lower than 10^{-4} [1]. Therefore, accurately predicting this destructive process is an important step to correctly assessing the ground impact risks of surviving fragments. However, the accurate prediction of re-entering fragments is a demanding and challenging task in itself, as it entails addressing a complex multi-physics problem that includes heat transfer calculations, aerodynamic and aerothermodynamic load computations for different flow regimes, and structural dynamics and fragmentation analysis.

During re-entry, the bodies will experience various degrees of flow rarefaction, which can be reliably simulated using high-fidelity techniques such as CFD and DSMC when applied to the suitable regime. However, high-fidelity simulations are computationally demanding, even more with increasingly complex assumptions and increasing number of fragments through the demise process, making the use of low-fidelity methods appealing. Several re-entry tools have been developed to address the multi-disciplinary simulation, including SCARAB (ESA/HTG) [2], PAMPERO (CNES) [3] and MUSIC/FAST (ONERA) [4]. These tools use hypersonic local panel inclination methods based on the modified Newtonian theory for the continuum regime [5] and analytical methods based on the Schaaf and Chambre flat plate model [6] for the free-molecular regime. A bridging function connecting the continuum to the free molecular regime is used to obtain the necessary loads in the transitional regime [7].

Most of the re-entry tools use solemnly low-fidelity methods, however these are associated with a high degree of uncertainty arising from the simplified physical thermo-structural assumptions and the treatment of the objects' computational geometry. Furthermore, most currently available low-fidelity approaches do not account for the influence of shock-generated flow characteristics and shock impingement in the dynamics and fragmentation of bodies [8], increasing simulation uncertainty.

For the reentry simulations, a multi-fidelity based approach using TITAN multi-disciplinary tool [9, 10] is proposed. The uncertainty in the simulation results is reduced by using the high-fidelity solvers SU2-NEMO [11] for the continuum and slip regimes, and the SPARTA[12] (Stochastic PArallel Rarefied-gas Time-accurate Analyser) Direct Simulation Monte Carlo (DSMC) solver for the transitional and rarefied regimes. The SU2-NEMO CFD solver is used with automatic mesh generation and anisotropic mesh adaptation to sharply capture the complex flow interactions and accurately compute their influence on the overall simulation. Dynamic grid adaptation is also performed when SPARTA is

referenced, to adjust the grid cell sizes to the current density distribution.

To perform fast re-entry simulations while ensuring a satisfactory degree of confidence in the trajectory predictions, a trade-off between high- and low-fidelity models must be achieved. The selection of a criterion for automatically switching between low-fidelity and high-fidelity modelling becomes critical. If too many calls to the high-fidelity model are performed, the re-entry simulation becomes computationally expensive and time-consuming. On the other hand, a reduced number of calls may not decrease the simulation uncertainty adequately. Optimally, the high-fidelity tool should be utilised only when necessary to address the phenomena that are not resolved by low-fidelity tools, or to correct the loads applied in the re-entering objects for flow regimes with higher degree of uncertainty, increasing the confidence in the overall simulation process.

The current research is intended towards the development and implementation of an automatic switching criteria to change between low-fidelity and high-fidelity methods during the re-entry simulation. The proposed switch criteria is focused on increasing the simulation accuracy in the presence of multiple bodies, through the development of a shock envelope method derived from the work of Billig [13]. The use of a shock envelope allows to assess the boundaries of the shocks generated by the fragments which can impact the neighbour objects dynamics. Ultimately, the developed approach allows to increase the results accuracy when compared to the strict use low-fidelity models, allowing to reference high-fidelity tools in key time intervals. Therefore, the automatic fidelity trigger allows to reduce the number of calls of the high-fidelity tool and to reduce the uncertainty related to the formation of flow features derived from shock interaction in the presence of multiple fragments. The methodology described in this paper can be used for all the flow regimes encountered during re-entry. However, Billig's formula does not account for the level of flow rarefaction [14], requiring the use of correction factors. For the purpose of demonstration and validation, only the continuum regime is considered for the simulations.

This paper is organized as follows: Section II introduces the TITAN logic for the computation of the aerodynamic and aerothermodynamic loads, together with the governing equations and physical models used by the high- and low-fidelity methods within TITAN. Section III provides an overview of the formulation used for the generation of the shock envelope. Section IV highlights the methodology implementation within TITAN, together with the criteria used to switch between low- and high-fidelity methods. Section V shows a test-case regarding the reentry of the ATV satellite which fragments at an altitude of 78 km, showcasing the usability and usefulness of the methodology described in the previous sections. In Section VI, the main conclusions and future work are summarized.

2. MULTI-FIDELITY AEROTHERMODYNAMICS

The present multi-fidelity framework incorporated in TITAN enables the computation of aerodynamic and aerothermodynamic loads using fast simplified engineering models and accurate high-fidelity CFD/DSMC solvers. The low-fidelity models under consideration allow for the computation of the aerodynamic and aerothermodynamic quantities at the various flow regimes encountered by the bodies during the re-entry process (e.g. rarefied, transitional, slip-flow and continuum regime) using local panel inclination method based on the Modified Newtonian Theory. Additionally, the framework can calculate and use local radius information to improve surface heating prediction.

The high-fidelity simulations are computed using the CFD solver SU2-NEMO for the continuum regime and DSMC solver SPARTA [12] for the transitional and free-molecular regime. The use of CFD solvers require the generation of a grid capable of sharply capturing the flow features inside the computational domain. Therefore, before proceeding to the flow simulation, the tool automatically generates a numerical grid used to simulate the flow around the bodies. To achieve a grid-converged solution, anisotropic grid adaptation of the volume mesh and the generation of refined prismatic boundary layers is done to enable the physical surface heating accurate computation using the CFD solver. Similarly, the use of SPARTA DSMC solver requires the generation of uniform Cartesian grids to perform particle collisions and sampling of macroscopic properties, with cell sizes that are less than that of the local mean free path. Dynamical grid adaptation is automatically set up during the simulation run to ensure local cell size requirements. The generation and manipulation of the computational domain for both CFD and DSMC solvers is performed with resource to third-party tools, referenced inside the TITAN re-entry simulation framework. The flowchart for both low-fidelity and high-fidelity aerothermodynamic computation methods is showcased in Fig. 1.

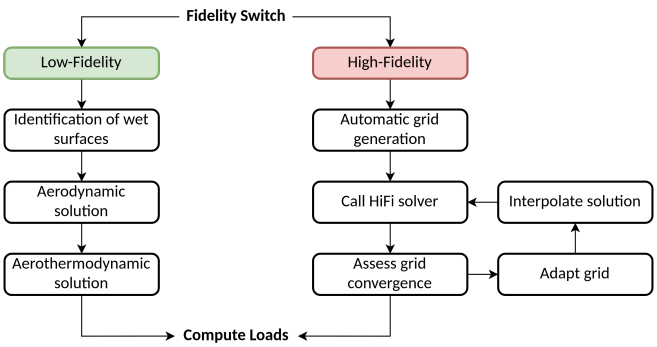

Fig. 1: Flowchart of the multi-fidelity aerothermal modelling.

Although low-fidelity methods are preferable for re-entry simulations due to their low computational cost, they use sim-

plified assumptions. Therefore, they may lead to incorrect predictions for objects with complex shapes, for flow regimes associated to high uncertainty (i.e. transitional regime), and for simulations where the presence of multiple bodies generate several shock waves that can impact the dynamics and structural integrity of neighbour objects. In these situations, the use of high-fidelity methods is advised to adequately resolve the flow conditions surrounding the objects. The implementation of an automatic switch to choose between low- and high-fidelity methods allows to reach a compromise between speed and accuracy, while allowing to appropriately resolve the scenarios that the strict use of low-fidelity models cannot. Additionally, high-fidelity methods can also be referenced to validate physical events triggered by low-fidelity models.

The multi-fidelity within TITAN is not limited to the aerodynamics and aerothermodynamic computation. In fact, TITAN also utilizes a multi-fidelity approach for the computation of structural dynamics. This is achieved by the use of the third-party open-source tools FEniCS[15] and Peridigm[16], which allow to compute the displacement and stress using a finite element and peridynamics formulation, respectively. Within the multi-fidelity approach, FEniCS is used to quickly compute the objects stress and displacement derived from the applied aerodynamic loads. If yields stress is reached and fragmentation is in imminence, Peridigm is then used to adequately verify if the applied loads are sufficient for fragmentation to occur.

2.1. SU2-NEMO

Over the years, the urging requirement to simulate chemically-reactive multi-species and non-equilibrium flows led to the development of SU2-NEMO (NonEquilibrium MOdels solver). The closure of the governing equations for the system of interest is achieved through the linkage of SU2-NEMO and the thermochemistry library Mutation++ [17] (Multicomponent Thermodynamic And Transport properties for IONized gases in C++). The library contains efficient algorithms for the computation of the required mixture properties, such as thermodynamic, transport and chemical kinetic gas properties for a wide range of temperatures.

The system of governing equations is obtained through the extension of the Navier-Stokes equations to account for chemically-reacting, nonequilibrium flows, using the two-temperature model by Park. The translational and rotational energy mode are assumed to be at equilibrium with one another. The same approach is used for the vibrational and electronic energy mode. The system can be described as:

$$\frac{\mathrm{d}\mathbf{U}}{\mathrm{d}t} + \nabla \cdot \mathbf{F^i}(\mathbf{U}) = \nabla \cdot \mathbf{F^v}(\mathbf{U}) + \mathbf{Q}(\mathbf{U}), \qquad (1)$$

where $\mathbf{U}$ are the conservative variables, $\mathbf{Q}$ are the source terms, $\mathbf{F^i}$ and $\mathbf{F^v}$ are the inviscid and viscous fluxes, respectively. The vectors are given by

$$\mathbf{U} = \begin{Bmatrix} \rho_1 \\ \vdots \\ \rho_{n_s} \\ \rho\mathbf{u} \\ \rho e \\ \rho e^{\text{v-e}} \end{Bmatrix}, \quad \mathbf{F^i} = \begin{Bmatrix} \rho_1\mathbf{u} \\ \vdots \\ \rho_{n_s}\mathbf{u} \\ \rho\mathbf{u}\otimes\mathbf{u} + p\bar{I} \\ \rho\mathbf{u}h \\ \rho\mathbf{u}e^{\text{v-e}} \end{Bmatrix},$$

$$\mathbf{F^v} = \begin{Bmatrix} \mathbf{J}_1 \\ \vdots \\ \mathbf{J}_{n_s} \\ \bar{\tau} \\ \bar{\tau}\cdot\mathbf{u} + \sum_s \mathbf{J}_s h_s + \mathbf{q}^{\text{t-r}} + \mathbf{q}^{\text{v-e}} \\ \sum_s \mathbf{J}_s h_s^{\text{v-e}} + \mathbf{q}^{\text{v-e}} \end{Bmatrix}, \quad \mathbf{Q} = \begin{Bmatrix} \dot{\omega}_1 \\ \vdots \\ \dot{\omega}_{n_s} \\ 0 \\ 0 \\ \dot{\Omega} \end{Bmatrix}, \qquad (2)$$

in which ρ is the density, $\mathbf{u}$ is the velocity vector, p is the static pressure, h is the total enthalpy per unit mass of the mixture, e is the energy per unit mass, $\bar{\tau}$ is the viscous stress tensor, $\mathbf{q}$ is the conduction heat flux, $\mathbf{J}$ is the mass diffusion flux, $\dot{\omega}$ is the net rate of species production, $\dot{\Omega}$ is the source term of vibrational energy and n_s is the number of species in the mixture. The subscript index s stands for the s^{th} chemical species in the mixture and the superscript t-r and v-e stand for the translational-rotational and vibrational-electronic modes, respectively. If the quantity does not have a superscript, it is related to the full mixture. The term $\bar{I}$ denotes the identity matrix.

2.2. SPARTA-DSMC

Direct Simulation Monte Carlo (DSMC) is a particle-based simulation technique proposed by G.A.Bird [18] for the stochastic simulation of the Boltzmann equation. It models dilute gas flows using simulated molecules that represent a large number of real molecules. The main idea of the method is to solve the collision term of the Boltzmann equation using a probabilistic approach to reproduce the statistical behaviour of real molecules. This is accomplished by decoupling deterministic molecule motion from probabilistic intermolecular collisions over short time intervals. Grid cells are used to discretise the physical space to select local collision pairs probabilistically and sample the macroscopic properties using relations from the kinetic theory of gases. As a consequence, the cell size and the time step must be smaller than the mean free path and the mean collision time, respectively [19]. Since the number of simulated molecules in a grid cell vary during the simulation run, macroscopic properties are obtained by sampling the simulated molecules data over a large number of time steps after reaching the steady state.

Sandia's open-source parallel DSMC code SPARTA is used in TITAN to account for high-fidelity simulations in the transitional and rarefied regime. SPARTA discretises the computational domain into a hierarchical, multi-level Cartesian grid which is used to track simulated molecules, perform

collisions and chemistry operations. Dynamic grid adaptation based on the local flow properties can be performed to improve the simulation accuracy while reducing the computational cost. The variable-hard-sphere (VHS) or the variable-soft-sphere (VSS) [18] interaction model is used to model binary collisions between the molecules while the Larsen-Borgnakke model is used to model the energy exchange between internal modes of the molecule. During particle collisions, gas-phase chemical reactions can be carried out using Bird's Total Collision Energy (TCE) [20] or Quantum-Kinetic (QK) models [21]. The gas-surface interactions (GSI) are modelled using Maxwell or the Cercignani-Lampis-Lord model (CLL) [22] that use accommodation coefficients as inputs.

The multi-fidelity methodology in TITAN can automatically create the input script that can be utilized to run high-fidelity SPARTA-DSMC simulations for specific flow conditions during the re-entry trajectory. These simulations can be computationally expensive and should be used optimally. The current study's key research contribution is the application of switching criteria based on Billig's empirical expression to predict the shape and position of shock waves. As previously stated, this expression does not account for rarefaction effects when predicting diffused shock waves in rarefied hypersonic flows [23]. It has already been established that rarefaction effects cause the shock wave's position to deviate significantly [14] from that predicted by Billig's empirical formula. Therefore, the automatic fidelity switching criteria for rarefied hypersonic flows is beyond the scope of the current study and will be investigated in a future study.

2.3. Low-fidelity models

The low-fidelity aerodynamic and aerothermodynamic models use the local panel inclination methods for hypersonic flow, enabling a rapid computation of the loads applied to the multiple fragments during atmospheric re-entry. The aerodynamics in the continuum regime ($K_n \leq 10^{-3}$) is estimated with the Modified Newtonian Theory [5] while for the free-molecular regime ($K_n \geq 10^2$) it is computed using the Schaaf and Chambre [6] model for an inclined flat-plate. The pressure and shear stress contributions from each of the facets are computed as a function of local flow inclination angle (θ). Additionally, the shear stress contribution in the continuum regime is considered to be negligible.

For the aerothermal heating estimation in the continuum regime, several analytical heat transfer correlation models like Fay-Riddell [24], Kemp-Detra-Riddell [25] and Van Driest model [26] are employed, enabling the assumption for both non-catalytic and fully-catalytic wall boudary conditions. For the rarefied regime, Schaaf and Chambre flat plate theory is used. A local radius formulation is used to increase the accuracy of the aerothermodynamics computation of blunt nosed and sharp-edged bodies.

In the transitional regime, the aerodynamics is estimated through the use of generalized aerodynamic bridging functions as described in [9, 10]. For the calculation of the aerothermodynamic properties in the transitional regime, a dedicated bridging model similar to the model developed by Alessandro et al. [27] has been integrated into TITAN, see Ref. [9, 10]. The integrated bridging function was developed using different re-entry heating data with distinct local nose radius to shift from a radius/inclination-based model in the near-continuum regime to a pure inclination-based model in the free-molecular regime. The reason being that, in the continuum regime, the heat flux is computed as a function of the local radius and panel inclination, while in the free-molecular regime, the thermal computation is radius independent.

3. SHOCK ENVELOPE

The presence of neighbour objects in supersonic and hypersonic regimes can generate shock waves that have an impact on the following fragments. An example is shock impingement, where the shock impinges the surface of following bodies, leading to highly-localized aerothermal loads that impact the dynamics and the structure of the object, which cannot be fully resolved using low-fidelity methods. In order to detect if the presence of multiple bodies in the re-entry simulation give rise to such flow features that require the use of high-fidelity tools to be captured, it is necessary to estimate the shock position generated by the fragments.

There are analytical methods to estimate the shock position for simple geometries, such as tangent wedge/cone method and shock expansion theory for attached shocks [28] and Billig hyperbola formula for detached shocks [13]. However, for bodies with complex shapes, the vast majority of the methods developed for shockwave detection require the post-processing of the solution obtained from CFD/DSMC tools [29]. For re-entry simulations, the shock position has to be estimated at every time-iteration, thus the ability of quickly estimating the shock location without relying on high-fidelity tools would significantly reduce the computational cost.

Despite the fact that accurate shock estimation is difficult in the case of intricate geometries, it is possible to compute a shock envelope with a low computational cost. By definition, the shock envelope must contain the shock generated by the object itself. This approach allows to formulate a switch criteria using the relative position of the objects with respect to the shock envelope of neighbour objects. Thus, when a fragment is inside a shock envelope, high-fidelity tools are called.

This section proposes the use of Billig's formula to generate the shock envelope. An example of a similar approach was done in the work of Catalano [30], where Billig's expression was used to limit the computational domain over a Vega launcher in supersonic regime. This method assumes that the detached shockwave generated by a sphere can be written as a hyperbolic function, asymptotic to the freestream Mach angle

or, in the case of a cone or wedge, to the attached shock angle θ. The expression formulated by Billig is given as

$$x = R + \Delta - R_c \cot^2\theta \left[\left(1 + \frac{r^2 \tan^2\theta}{R_c^2} \right)^{1/2} - 1 \right] \quad (3)$$

being R the radius of curvature of the geometry at the stagnation point, R_c the radius of curvature of the shock at the vertex, Δ the stand off distance and θ the asymptotic angle of the hyperbola. The stand off distance and vertex radius of curvature are given by the empirical relation proposed in the work of Ambrosio and Wortman in the continuum regime [31] and are respectively formulated as

$$\frac{\Delta}{R} = 0.143 \exp\left(\frac{3.24}{M_\infty^2} \right) \quad (4)$$

$$\frac{R_c}{R} = 1.143 \exp\left(\frac{0.54}{(M_\infty - 1)^{1.2}} \right) \quad (5)$$

where M_∞ is the free-stream Mach number. Billig's formula is only dependent on the free-stream Mach number and the radius of the sphere, and does not take into consideration the level of flow rarefaction, as stated in the research of Nicolas et al. [14], where the authors have verified that with the increase in the Knudsen number, the stand off distance given by the empirical formula further deviates from the experimental results. Therefore, for this research, the conducted simulations are performed in the continuum regime.

4. DEVELOPMENT OF A FIDELITY SWITCH FOR MULTIPLE BODIES SIMULATION

The vast majority of spacecraft-oriented tools are based on low-fidelity models to conduct the simulation of the re-entry process. While TITAN enables the use of engineering models, it is not restricted to engineering methods. The multi-fidelity framework can also reference high-fidelity tools, according to the imposed level of compromise between accuracy and computational power.

An important key event in determining the dynamics of the objects is during breakup events. TITAN enables for the specification of a time window duration to run high-fidelity tools in order to assess the initial dynamics after breakup, for all the fragmentation scenarios occurring during the re-entry process. However, the time window strategy does not allow to assess when fragments cease to be impacted by the shock generated by neighbour objects.

To account for the relative position of the bodies, an automatic fidelity switch criteria to choose between low- and high-fidelity models has been developed and integrated in the framework of TITAN, using an approach based on Billig's shock estimation for a sphere. Billig's formula enables the formulation of an analytical equation for the creation of a shock envelope, which can be used as a criteria to choose between the different fidelity methods in a fast and computationally inexpensive way. In order to generate the shock envelope using Billig's formulation, a virtual equivalent sphere needs to be considered. As an additional remark, all the procedures definitions in the following sections are performed in the wind frame, i.e. the X-axis of the referential frame is aligned with the flow.

The location of the sphere center is computed such that the y- and z-coordinates are equal to the y- and z-coordinates of the mid-point between the maximum and minimum vertex coordinates of the object analysed. The x-coordinate of the sphere center is equal to the minimum x-coordinate of the body. The radius of the sphere is computed such that it corresponds to the minimum radius possible to encompass the object in the YZ view plane, with the sphere center at the already computed position. Afterwards, the shock envelope can be computed using the Billig's formula. An example of this approach is shown in Fig. 2.

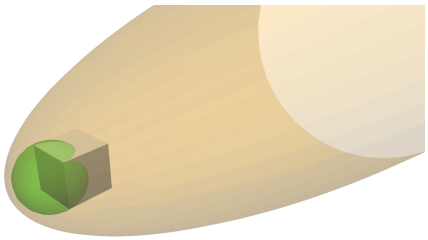

Fig. 2: Visualization of the virtual sphere and the equivalent shock envelope for a cube geometry.

The approach is tested against two cases of a Mach 10 flow, using as geometries a cube and a cylinder, which can be visualized in Fig. 3 and 4, respectively. The shock envelope generated by the equivalent sphere is able to contain the shock generated by the object for both cases, thus showcasing the capabilities of using the same formulation for complex geometries. As it can be observed for Fig. 4b, the proposed approach is conservative for elongated bodies in the Y- and Z- direction, while it is closely matching the shock in Fig. 4a, where the cylinder is elongated in the flow direction. This difference is due to the approach used to generate the virtual sphere, which has to include the entire object in the YZ plane perspective.

Due to the nature of the hyperbolic formula derived by Billig, it is possible to rewrite Eq. 3 for a sphere with an arbitrary position in the wind frame. For a body i with an equivalent sphere with center at (x_{s_i},y_{s_i},z_{s_i}), and assuming the flow direction to be in the positive X-axis direction, the hyperbolic formula for the shock envelope can be rewritten as

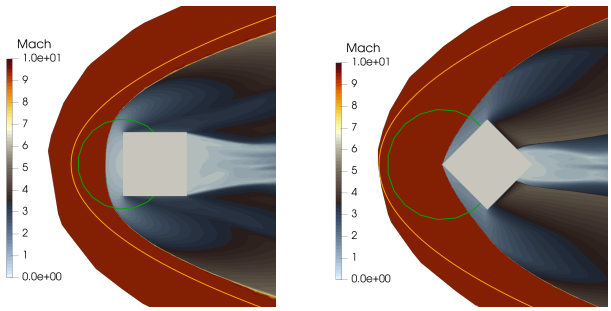

(a) Cube with 0° inclination. (b) Cube with 45° inclination.

Fig. 3: Shock envelope for cubic geometry at Mach 10

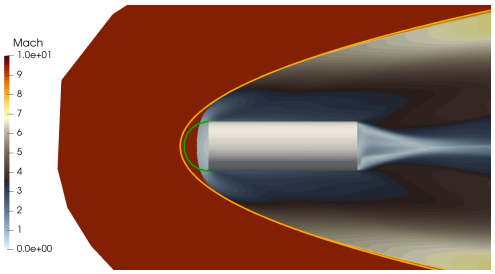

(a) Cylinder with revolution axis parallel to the flow direction.

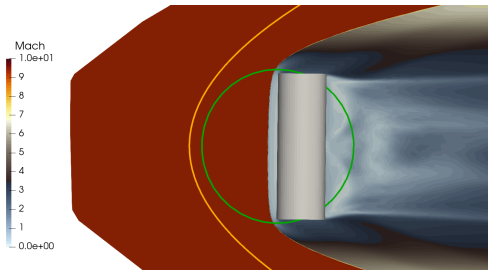

(b) Cylinder with revolution axis normal to the flow direction.

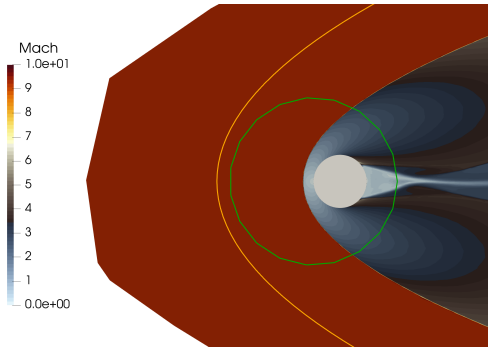

(c) Cylinder with revolution axis normal to the flow direction.

Fig. 4: Shock envelope for cylindrical geometry at Mach 10

$$(x - x_{s_i}) = -R_c - \Delta + R_c \cot^2\theta \times \left[\left(1 + \frac{(r - r_{s_i})^2 \tan^2\theta}{R_c^2}\right)^{1/2} - 1\right] \quad (6)$$

where r is defined as

$$r = \sqrt{y^2 + z^2}. \quad (7)$$

Rearranging equation 8, the inner side of the hyperbola, which defines the shock envelope, can be defined as

$$R_c \cot^2\theta \left[\left(1 + \frac{(r - r_{s_i})^2 \tan^2\theta}{R_c^2}\right)^{1/2} - 1\right] \geq -(R_c + \Delta). \quad (8)$$

For a given body j, with $i \neq j$, the coordinates of the k_{th} vertex of the body are given as (x_{j_k},y_{j_k},z_{j_k}). If any of the vertexes is inside the hyperbola, CFD tools are used to compute the aerothermal loads. Otherwise, if all the vertex are outside the hyperbola, low-fidelity methods are used. In other words, high-fidelity methods are used if a single vertex complies with the following criteria:

$$(x_{j_k} - x_{s_i}) - R_c \cot^2\theta \left[\left(1 + \frac{(r_{j_k} - r_{s_i})^2 \tan^2\theta}{R_c^2}\right)^{1/2} - 1\right] \geq -(R_c + \Delta), \quad \text{for k = 0, 1, ..., N.} \quad (9)$$

An illustrative example of the proposed methodology for the fidelity switch criteria is presented in Fig. 5, where the vertexes inside the envelope are flagged. Therefore, in this example, if any of the fore-sphere vertexes are inside the shock envelope generated by the leading sphere, high-fidelity tools are used for the computation of the surface loads. The considered approach not only allows to account for objects leaving the shock envelope, but also for fragments re-entering it, thus eventual interaction with the shock generated by a leading fragment can be expected.

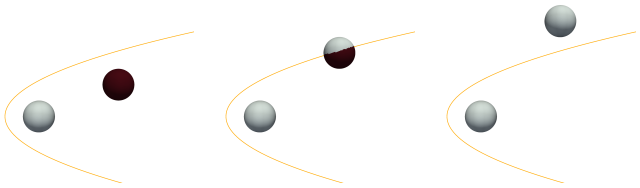

Fig. 5: Representation of the sphere positioning in relation to the shock envelope.

Some fragments may not able to leave the shock generated by the leading object, thus not leaving the shock envelope. From the methodology described so far, this would imply that the high-fidelity tools would be referenced at every time iteration, leading to high computational costs. To prevent this, it is important to enclose the shock envelope longitudinally, but the selection for the enclosing criteria is complex and subject to future research. For this work, only the envelope criteria generated by Billig's formula is considered.

5. ATV SATELLITE RE-ENTRY

In order to demonstrate the multi-fidelity capabilities of TITAN with the automatic fidelity switch presented in this work and assess its impact on the dynamics of the fragments, a conceptual ATV re-entry test-case without thermal ablation was conducted. A previously conducted work [9] has already demonstrated the existence of discrepancies between high-fidelity and low-fidelity methods instants after the fragmentation of the joints connecting the main body and the solar panels due to shock influence. The initial trajectory conditions and fragmentation trigger used in this simulation are summarised in Table 1 and the initial simplified ATV geometry before the breakup is shown in Fig. 6.

Table 1: Initial trajectory conditions and geometry details.

Parameter	Value
Altitude [km]	120
Velocity [km/s]	7.57
Flight path angle [°]	-1.45
Initial pitch angle velocity [°/s]	10
Fragmentation trigger altitude [km]	78
Number of facets [$\times 10^3$]	40
Time step [s]	0.25

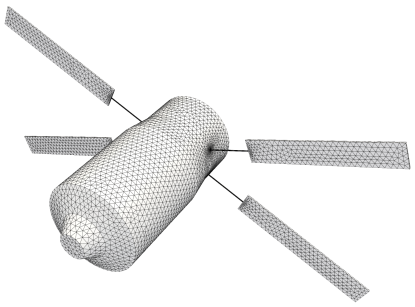

Fig. 6: Geometry configuration of the conceptual ATV geometry.

Up until the moment of fragmentation at 78 km, TITAN uses low-fidelity models to compute the surface loads. The ATV trajectory up until fragmentation can be visualized in Fig. 7

At the moment of fragmentation ($t = 171.95s$), the objects are re-entering at Mach 26, leading to the formation of shock-waves. Using the methodology described in Sec. 4, it is possible to estimate if the fragments are subjected to the influence of the shock generated by leading objects, requiring the use of high fidelity methods for accurate predictions of surface loads. The forces and moments applied to the fragments were computed for a time interval of $\Delta t = 2.0s$ using a time-step of $dt = 0.05s$ for both low- and high-fidelity methods to compare the differences.

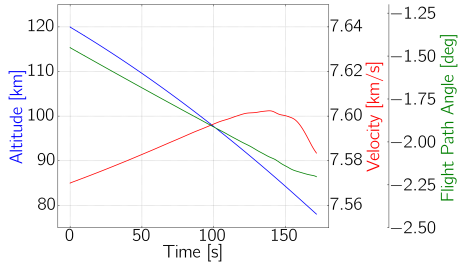

Fig. 7: ATV trajectory profile before breakup.

The results shown in Fig. 8 illustrate the forces and moments experienced by a single solar panel. The plots show results for both low and high-fidelity models. The blue background indicates the time interval where the fragment is inside a shock envelope generated by the main body or leading panels, thus requiring the use of high-fidelity tools, and the yellow background indicates the time interval where the fragment is not interacting with any shock envelope, thus low-fidelity models can be used. As it can be verified, the difference in the methods is more pronounced when the fragment is inside the shock envelope due to the influence of the leading body. As the fragment leaves the shock envelope, the forces and moments computed using both methods become comparable as there is no further interaction with shock waves. Therefore, after exiting the envelope, low-fidelity methods are enough to capture the object's dynamics adequately.

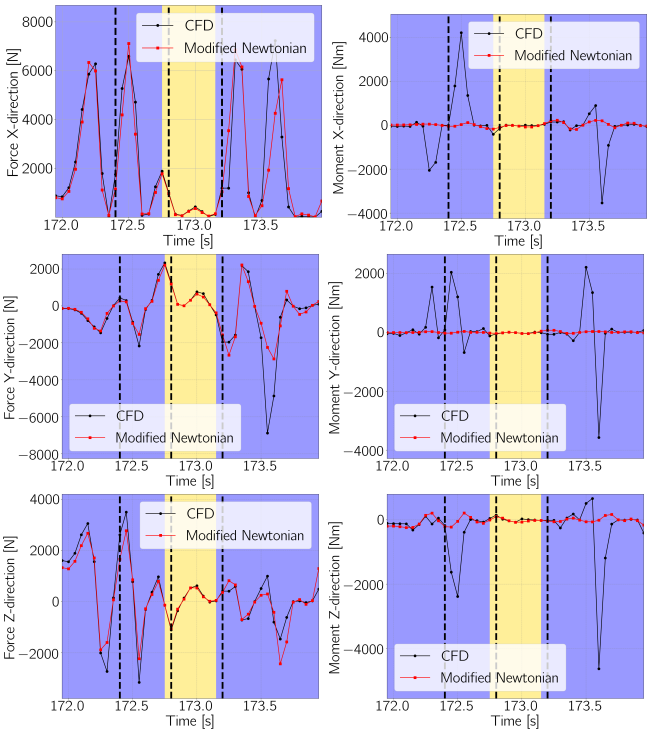

Fig. 8: Solar panel forces and moments comparison.

Three different scenarios were sequentially identified in Fig. 8 by a black dashed line. After fragmentation of the joints, due to the proximity of the solar panels and the main body, high-fidelity methods are required to fully capture the loads applied in the fragments, as visualized in Fig. 9. Afterwards, the tracked solar panel leaves the shock influence of the remaining fragments. At this stage, TITAN is able to separate the fragments whose dynamics can be captured using Modified Newtonian from the fragments that require the generation of a numerical grid to run a CFD/DSMC simulation. The fragment selection process enables to reduce the number of objects in the high-fidelity simulation, thus minimizing the computational cost. This scenario, illustrated in Fig. 10, is similar to the one represented by the yellow background, where the forces and moments using both low and high fidelity are in good agreement. Lastly, a scenario was observed where different clusters of fragments were not interacting with other clusters, but the shock influence was noticeable inside both clusters, requiring the use of high-fidelity models. TITAN can separate the fragments that are interacting with each other into separate clusters according to the generated shock envelope . Therefore, the shock-waves generated from the fragments associated to a cluster do not interact with other clusters, as it can be verified in Fig. 11, TITAN is able to run separate high-fidelity simulations, reducing the time and complexity of the flow computation. The panel used for the comparison in Fig. 8 is circled in red.

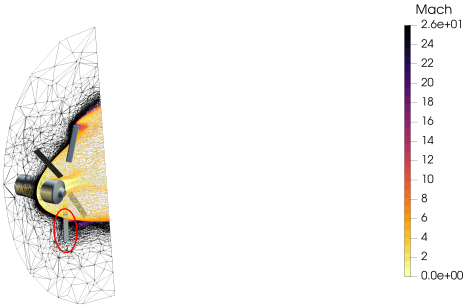

Fig. 9: Full CFD simulation at $t = 172.4s$ using one cluster.

The proposed conservative method ensures that the objects outside the shock envelope hyperbola do not interact with leading shocks. Therefore, it is expected for the forces and moments computed by both CFD and Modified Newtonian method to be similar. The use of an analytical function to assess the position of the objects with respect to the generated shock envelops allows to quickly assess the level of fidelity required to adequately compute the applied loads at the given instant of time.

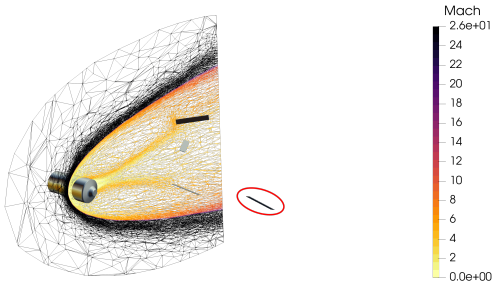

Fig. 10: Fidelity separation at $t = 172.8s$. Low-fidelity model is used for the circled solar panel

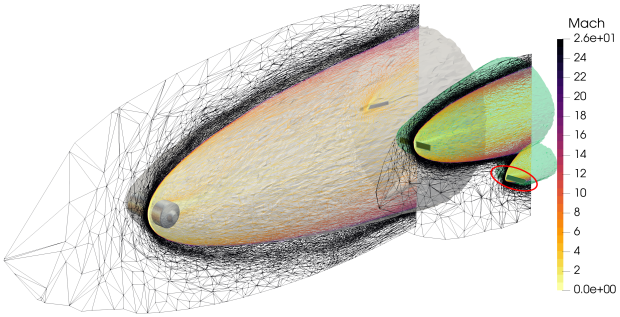

Fig. 11: Mach iso-surface for different clusters at $t = 173.3s$.

6. CONCLUSIONS

The current study aims to investigate an automatic fidelity switching criteria based on the creation of a shock envelope. Billig's empirical shock relation for a sphere is used to generate equivalent shock envelopes for various primitive objects to aid the development of a fidelity switch for multiple bodies simulation. The proposed methodology enables to automatically switch between the low-fidelity local-panel inclination methods and the high-fidelity Computational Fluid Dynamics (CFD) or Direct Simulation Monte Carlo (DSMC) techniques, such that the complex flow features resulting from the proximity of the bodies are adequately resolved to increase the confidence in the simulations. A conceptual re-entry test case scenario involving the Automated Transfer Vehicle (ATV) geometry is used to simulate the moments after the solar panels fragment from the main body of the ATV. A shock envelope criteria is used to assess the level of fidelity required at each time iteration and for each object analysed.

Acknowledgments

This research is supported by the European Space Agency MIDGARD project, ESA Contract No. 4000130436/20/NL/MH/ac, 2020-2023. This research is partially supported by the EU H2020 MSCA-ETN Stardust-R, grant agreement 813644.

7. REFERENCES

[1] J.-C. Liou, M. Kieffer, A. Drew, and A. Sweet, "The 2019 u.s. government orbital debris mitigation standard practices," *Orbital Debris Quarterly News*, vol. 24, no. 1, pp. 4–8, 2020.

[2] G. Koppenwallner, Bent Fritsche, T. Lips, and H. Klinkrad, "Scarab - a multi-disciplinary code for destruction analysis of space-craft during re-entry," *European Space Agency, (Special Publication) ESA SP*, vol. 563, pp. 281, 01 2005.

[3] Julien Annaloro, Pierre Omaly, Vincent Rivola, and Martin Spel, "Elaboration of a new spacecraft-oriented tool: Pampero," in *Proceedings of the 8th European Symposium on Aerothermodynamics for Space Vehicles*, 2015.

[4] Frédéric Sourgen, Ysolde Prévereaud, J. l. Verant, Emmanuel Laroche, and Jean-Marc Moschetta, "Music/fast, a pre-design and pre-mission analysis tool for the earth atmospheric re-entry of spacecraft, capsules and de-orbited satellites," in *Proceedings of 8th European Symposium on Aerothermodynamics for Space Vehicles, 2 March 2015 - 6 March 2015 (Lisbonne, Portugal*, 2015.

[5] Lester Lees, "Hypersonic flow," *Journal of Spacecraft and Rockets*, vol. 40, no. 5, pp. 700–735, 2003.

[6] Samuel A. Schaaf and Paul L. Chambre, *Flow of Rarefied Gases*, Princeton University Press, 1958.

[7] Luigi Morsa, Gennaro Zuppardi, Antonio Schettino, and Raffaele Votta, "Analysis of bridging formulae in transitional regime," *AIP Conference Proceedings*, vol. 1333, 05 2011.

[8] Julien Annaloro, Stéphane Galera, P.Kärräng, Ysolde Prevereaud, Jean-Luc Vérant, Martin Spel, Pierre Van Hauwaert, and Pierre Omaly, "Space debris atmospheric entry prediction with spacecraft-oriented tools," 04 2017.

[9] Fábio Morgado, Sai Abhishek Peddakotla, Catarina Garbacz, Massimiliano L. Vasile, and Marco Fossati, "Multi-fidelity approach for aerodynamic modelling and simulation of uncontrolled atmospheric destructive entry," 2022.

[10] Fábio Morgado, Sai Abhishek Peddakotla, and Marco Fossati, "A multi-fidelity simulation framework for atmospheric re-entering bodies," in *ESA Aerothermodynamics and Design for Demise (ATD3) Workshop*, 2021.

[11] Walter T. Maier, Jacob T. Needels, Catarina Garbacz, Fábio Morgado, Juan J. Alonso, and Marco Fossati, "SU2-NEMO: An Open-Source Framework for High-Mach Nonequilibrium Multi-Species Flows," *Aerospace*, vol. 8, no. 7, 2021, 10.3390/aerospace8070193.

[12] SJ Plimpton, SG Moore, A Borner, AK Stagg, TP Koehler, JR Torczynski, and MA Gallis, "Direct simulation monte carlo on petaflop supercomputers and beyond," *Physics of Fluids*, vol. 31, no. 8, pp. 086101, 2019.

[13] Frederick S. Billig, "Shock-wave shapes around spherical-and cylindrical-nosed bodies.," *Journal of Spacecraft and Rockets*, vol. 4, no. 6, pp. 822–823, 1967.

[14] Nicolas Rembaut, Romain Joussot, and Viviana Lago, "Aerodynamical behavior of spherical debris in the supersonic and rarefied wind tunnel marhy," *Journal of Space Safety Engineering*, vol. 7, no. 3, pp. 411–419, 2020, Space Debris: The State of Art.

[15] M. S. Alnæs, J. Blechta, J. Hake, A. Johansson, B. Kehlet, A. Logg, C. Richardson, J. Ring, M. E. Rognes, and G. N. Wells, "The FEniCS Project Version 1.5," *Archive of Numerical Software*, 2015.

[16] J.A. Mitchell M.L. Parks, D.J. Littlewood and S.A. Silling, "Peridigm Users' Guide," *Sandia National Laboratories*, 2012.

[17] J. Scoggins and T. Magin, "Development of mutation++: Multicomponent thermodynamic and transport properties for ionized plasmas written in c++," 06 2014.

[18] GA Bird, *Molecular gas dynamics and direct simulation Monte Carlo*, 1998.

[19] Zhi-Xin Sun, Zhen Tang, Ya-Ling He, and Wen-Quan Tao, "Proper cell dimension and number of particles per cell for dsmc," *Computers & Fluids*, vol. 50, no. 1, pp. 1–9, 2011.

[20] GA Bird, "Chemical reactions in dsmc," in *AIP Conference Proceedings*. American Institute of Physics, 2011, vol. 1333, pp. 1195–1202.

[21] GA Bird, "The qk model for gas-phase chemical reaction rates," *Physics of Fluids*, vol. 23, no. 10, pp. 106101, 2011.

[22] RG Lord, "Some further extensions of the cercignani–lampis gas–surface interaction model," *Physics of Fluids*, vol. 7, no. 5, pp. 1159–1161, 1995.

[23] MS Ivanov and SF1609761 Gimelshein, "Computational hypersonic rarefied flows," *Annual Review of Fluid Mechanics*, vol. 30, no. 1, pp. 469–505, 1998.

[24] J. Fay and F. R. Riddell, "Theory of stagnation point heat transfer in dissociated air," *Journal of the Aerospace Sciences*, vol. 25, pp. 73–85, 1958.

[25] R. W. Detra, "Addendum to heat transfer to satellite vehicle reentering the atmosphere," *Jet Propulsion*, vol. Dec., pp. 1256–1257, 1957.

[26] E. R. van Driest, "The problem of aerodynamic heating," *Aeronautical Engineering Review*, vol. 15, 10, pp. 26–41, 1956.

[27] Alessandro Falchi, Viola Renato, Edmondo Minisci, and Massimiliano Vasile, "Fostrad : An advanced open source tool for re-entry analysis," in *15th Reinventing Space Conference*, GBR, October 2017.

[28] John David Anderson, *Hypersonic and high temperature gas dynamics*, AIAA, 2000.

[29] Ziniu Wu, Yizhe Xu, Wenbin Wang, and Ruifeng Hu, "Review of shock wave detection method in cfd post-processing," *Chinese Journal of Aeronautics*, vol. 26, no. 3, pp. 501–513, 2013.

[30] P. Catalano, M. Marini, A. Nicolì, and A. Pizzicaroli, "Cfd contribution to the aerodynamic data set of the vega launcher," *Journal of Spacecraft and Rockets*, vol. 44, no. 1, pp. 42–51, 2007.

[31] Alphonso Ambrosio and Andrzej Wortman, "Stagnation-point shock-detachment distance for flow around spheres and cylinders in air," *Journal of the Aerospace Sciences*, vol. 29, no. 7, pp. 875–875, 1962.